

Photonic sensors for micro-damage detection: A proof of concept using numerical simulation

M. Sheyka¹, I. El-Kady^{2,3}, M. F. Su² and M. M. Reda Taha^{1*}

¹Dept. of Civil Eng., University of New Mexico, Albuquerque, NM 87131, U.S.A.

²Dept. of Electrical Eng., University of New Mexico, Albuquerque, NM 87131, U.S.A.

³Dept. of Photonic Microsystems Technologies, Sandia National Laboratories, Albuquerque, NM 87151, U.S.A.

(Received August 24, 2008, Accepted October 10, 2008)

Abstract. Damage detection has been proven to be a challenging task in structural health monitoring (SHM) due to the fact that damage cannot be measured. The difficulty associated with damage detection is related to electing a feature that is sensitive to damage occurrence and evolution. This difficulty increases as the damage size decreases limiting the ability to detect damage occurrence at the micron and submicron length scale. Damage detection at this length scale is of interest for sensitive structures such as aircrafts and nuclear facilities. In this paper a new photonic sensor based on photonic crystal (PhC) technology that can be synthesized at the nanoscale is introduced. PhCs are synthetic materials that are capable of controlling light propagation by creating a photonic bandgap where light is forbidden to propagate. The interesting feature of PhC is that its photonic signature is strongly tied to its microstructure periodicity. This study demonstrates that when a PhC sensor adhered to polymer substrate experiences micron or submicron damage, it will experience changes in its microstructural periodicity thereby creating a photonic signature that can be related to damage severity. This concept is validated here using a three-dimensional integrated numerical simulation.

Keywords: structural health monitoring (SHM); micro-damage detection; photonic crystal (PhC); finite difference time domain (FDTD).

1. Introduction

Structural health monitoring (SHM) represents the collective efforts of non-intrusive detection of damage in structures during operation. A significant challenge in SHM is the fact that damage cannot be measured (Sohn, *et al.* 2003, Worden and Dulier-Barton 2004) but can be inferred by realizing changes in mechanical features, e.g. strain magnitude, mode shape or signal energy (Doebeling, *et al.* 1996, Escobar, *et al.* 2005, Reda Taha, *et al.* 2006). This challenge in damage detection is magnified as the damage scale becomes smaller. Limited studies have been published on damage detection at the micron and submicron length scale of the material. Some challenges relate to the difficulty to probe materials at the micron/submicron scale and the significant level of noise associated with measurements at this length scale. While realizing damage at the micron/submicron length scale is not necessary for typical civil engineering structures (e.g. bridges), it becomes of value when damage detection is sought in critical structures such as aircrafts, space shuttles or nuclear storage tanks and structures. In these instances, damage diagnosis and prognosis at the micron/submicron scale can be an excellent

*Corresponding Author, E-mail: mrtaha@unm.edu

preventive measure for catastrophic events.

Application of monitoring techniques to critical structures like aircrafts has evolved into what is known as hot spot monitoring (Kessler and Spearing 2002). In such monitoring strategy only critical (hot) spots are monitored to realize damage evolution. Fig. 1 shows the hot spots on an aircraft where structural monitoring is necessary. The locations of these spots may be determined with the aid of finite element (FE) analysis. Moreover, locations where repair of cracks or surface damage took place are considered hot spots, while the actual repair of surface cracks using a composite patch prevents visual monitoring of crack propagation under the repair patch. Thus, a damage detection technique with a much higher resolution than that used in classical SHM is needed to monitor crack propagation at such spots. The challenge of detecting and quantifying damage in composites has been discussed by many researchers (Talreja 1994, Adams 2007). It is believed that micron and submicron damage detection techniques can be of great value for hot spot monitoring. Fig. 2 shows a schematic representation of a repaired crack using a composite patch and the location of a sensor above the repair patch for hot spot monitoring.

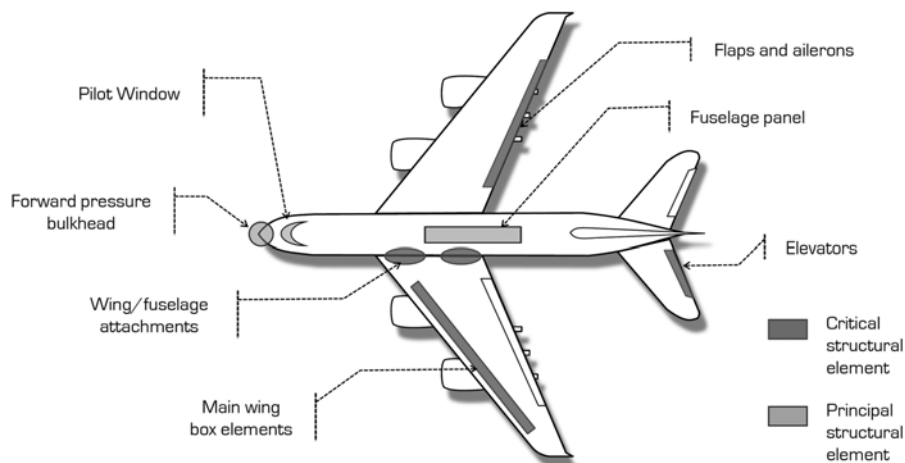


Fig. 1 Hot spot locations for monitoring a modern aircraft

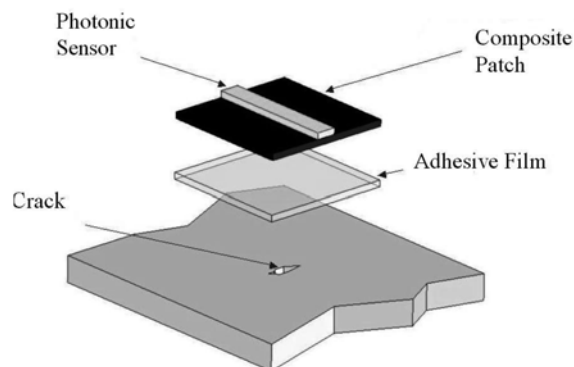


Fig. 2 Schematic representation of PhC sensor monitoring a micro-crack evolution in a structural composite repaired using composite patch technique

It is suggested that photonic sensors utilizing photonic crystals (PhC) technology is an effective way to monitor hot spots (Joannopoulos, *et al.* 1997, Fleming, *et al.* 2002). PhCs are synthetic materials fabricated at a periodicity length scale comparable to that of electromagnetic radiation, with micron and submicron features which control light propagation in three dimensions by opening a frequency gap where light cannot propagate (Lin, *et al.* 1998). A schematic representation of the geometry of three different PhCs is shown in Fig. 3. One-, two-, and three-dimensional photonic bandgaps have been produced by controlling one-, two- and three-dimensional microstructure of PhCs (Biswas, *et al.* 2003). The bandgap in PhC occurs as a result of the light waves undergoing destructive interference at certain combinations of frequencies such that photons with energy values corresponding to the bandgap cannot penetrate the lattice regardless of their angle of incidence. This occurs as a result of producing a well-defined repeating array of different refractive indices. An example bandgap of a PhC represented in the lattice space is shown in Fig. 4.

Given their unique properties, and the strong tie between the PhC microstructure periodicity and its photonic response represented by the bandgap profile, it is suggested that a photonic sensor using PhCs will be capable of detecting micron and submicron damage in materials. If adhered to the surface of a patch repair (or any surface of critical location of the structure), the PhC will deform as the substrate material experiences strains. If damage occurs, non-uniform strains will develop in the substrate resulting in non-uniform disturbance of the topology of the PhCs, thus disturbing the bandgap. This paper presents a methodology to verify this concept and to show how to relate the bandgap disturbance

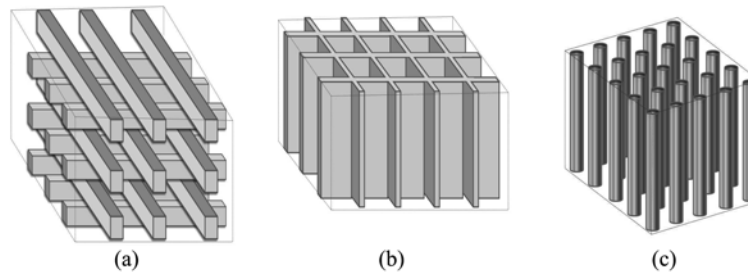


Fig. 3 Three representative PhCs showing its repetitive pattern

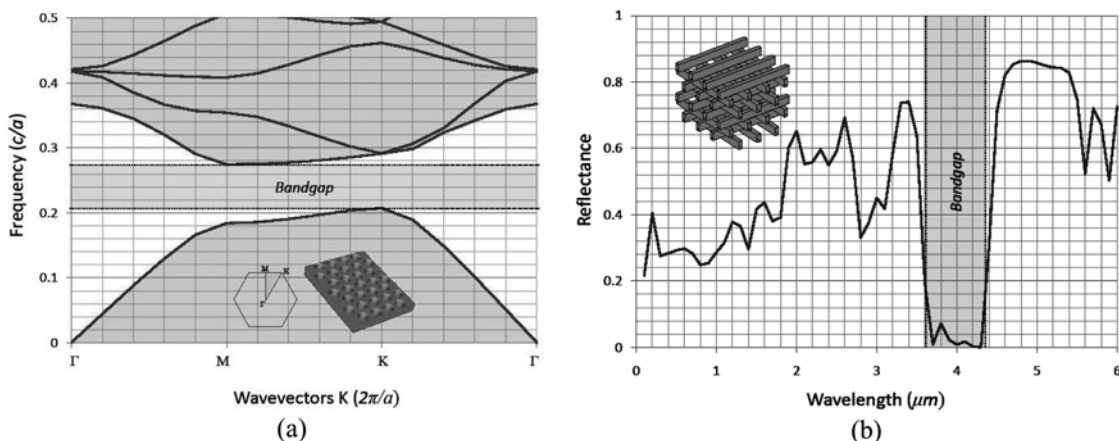


Fig. 4 Photonic bandgap of a PhC (a) lattice representation showing the bandgap with respect to lattice wave vector (b) reflection spectral shows a PhC where zero% reflectance (100% Transmission) is produced

to a quantifiable level of damage in the material.

An integrated simulation approach to prove the ability of a photonic sensor made of PhC to detect submicron damage in a substrate adhered to the photonic sensor is discussed. The first part of the paper discusses simulating the mechanical response of the PhCs using the FE method. The paper also presents the finite difference time domain (FDTD) method that is used to simulate the frequency spectrum of a PhC sensor. In addition, a computational geometry model to map the numerical grids simulating the PhC sensor in the FE method to the FDTD method is presented. The next step is to introduce a damage metric that relates changes in the reflectance spectra to micro-damage in the substrate material. In order to demonstrate the validity of using PhC sensors for micro-damage detection, a case study is presented.

2. Methods

2.1. Finite element (FE) modeling of PhC

A typical PhC consists of a periodic arrangement of inclusion “A” (e.g. silicon) in a matrix “B” (e.g. polymer). The objective of developing an FE model is to simulate the mechanical response of PhC to define the relative locations of the inclusions “A” and the matrix “B”. This is because of PhC photonic response is strongly tied to these relative locations. The FE method is a numerical method used to simulate mechanical behavior given a constitutive relation describing the material and a set of boundary conditions. A FE model thus discretizes a structure into nodes connected to one another through elements described by the constitutive models of the materials enclosed in these elements. The fundamental principle in FE is to relate the global forces vector $\{F_i\}$ to the global displacement vector $\{d_i\}$ by considering the global stiffness matrix $[K]$ (Logan 2002). This is described in Eq. (1).

$$\{F_i\} = [K] \cdot \{d_i\} \quad (1)$$

When modeling a PhC, the stiffness matrix $[K]$ is a function of the PhC topology, materials and geometry. Due to the complex geometry of a PhC, tetrahedral elements are utilized when meshing

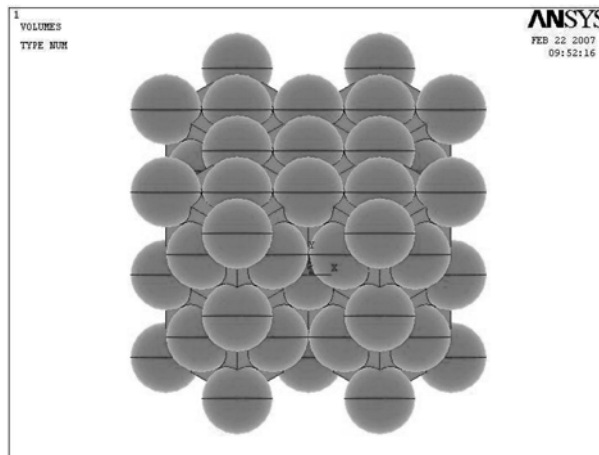


Fig. 5 A three-dimensional FE model of an inverse opal PhC

three-dimensional PhC, and triangular elements must be used in meshing two-dimensional crystals. An example of a FE model for an inverse opal PhC is shown in Fig. 5. The FE model of the PhC is developed such that it will be subjected to the strains at the location of the substrate where the PhC is adhered. The FE model output provides or generates the new deformed shape of the PhC with new relative locations of the matrix and inclusions. These new locations should be mapped to the FDTD method in order to simulate the photonic reflectance-frequency spectra of a PhC.

2.2. Finite difference time domain (FDTD) modeling of the PhC

Modeling the photonic response of PhC is critical in realizing the change in its reflectance spectra associated with the change in the periodicity of the PhC. There exist a number of modeling choices for performing the photonic simulation. For example, Sigalas, *et al.* (1996) recommended the Transfer Matrix Method (TMM) while work by El-Kady (2002) and Lin, *et al.* (2003) proposed the Modal Expansion Method (MEM). More recently, Ward and Pendry (1998) proved the ability to simulate the photonic response using the FDTD method. The TMM helps in computing the reflectance and transmittance of the PhC due to the principal light modes propagating in free space. However, the complexity of TMM calculations increases by the square of the mesh size, and hence the method is computationally expensive when a fine modeling grid is needed, as is the case of interest of this study. While MEM overcomes some of the computational problems with TMM by simulating the photonic response in the Fourier space, MEM convergence for a PhC under nonuniform strain requires many Fourier components, making the method computationally expensive.

Given the above limitations, the simulation of the photonic response of the PhC for damage detection applications was performed in this study using the FDTD method. The FDTD method introduces a solution of the Maxwell's equations by replacing the partial derivatives in Maxwell equations (Eqs. (2) and (3)) by finite differences ψ described by Eq. (4).

$$\nabla \Phi = \varepsilon_0 \varepsilon(\vec{r}) \frac{\partial E}{\partial t} \quad (2)$$

$$\nabla E = \mu_0 \mu(\vec{r}) \frac{\partial \Phi}{\partial t} \quad (3)$$

$$\Psi_j = \sqrt{\left(\frac{\partial x}{\partial \psi_j}\right)^2 + \left(\frac{\partial y}{\partial \psi_j}\right)^2 + \left(\frac{\partial z}{\partial \psi_j}\right)^2} \quad \vec{E} = \psi_j E_j, \quad \vec{\Phi} = \psi_j \Phi_j, \quad j = 1, 2, 3 \quad (4)$$

Where Φ is the magnetic field vector, E is the electric field vector, ε_0 and μ_0 are the free space permittivity and permeability constants, ε and μ are the permittivity and permeability of the PhC sensor. ψ_i and Ψ_i are space coefficients and vectors for a generalized coordinate system, \vec{r} is the direction vector that represents the directionality of the field, and t is time. Using the appropriate initial and boundary conditions, it is possible to obtain the electric and magnetic fields as a function of time. To obtain the transmission and reflection coefficients, a Fourier transform is applied while considering the field data as principal light modes propagating in free space. Published literature indicated that FDTD has proven to be very efficient in simulation of very complex structures (El-Kady, *et al.* 2008).

2.3. Integrated simulation using computational geometry

To simulate the process of micro-damage detection and quantification using PhCs, the two computational approaches described earlier are integrated; the FE and the FDTD methods. The FE method is used to simulate microstructural disturbances in the PhC as a result of micron or submicron damage in the substrate material. The FDTD method simulates the photonic spectral response of the PhC sensor with both normal (healthy) substrate and when damage occurs in the substrate. The challenge lies in the fact that the modeling grid used to describe the PhC in FDTD model is different than that used to describe the PhC in the FE model. The integration between the two methods requires linking the two grid/meshing systems. This is a fundamental step to accurately simulate the multi-physics of PhC and their use for micro-damage detection. Fig. 6(a) shows the two different grid systems used in FE and FDTD. It is suggested that a computational geometry module can be used to map the two grid systems.

The essence of the proposed approach can be explained by considering point “q” in space with coordinates (q_1, q_2, q_3) as shown in Fig. 6(b). To test whether a point “q” in space resides inside a tetrahedron or not, two steps are required. First, a box surrounding the tetrahedron of interest is created to exclude points that are definitely outside the tetrahedron (O’Rourke 1998). The coordinates of the tetrahedron are compared to the bounding box coordinates. If a point is outside the bounding box, then it resides outside the tetrahedron. If the point is inside the bounding box, a second process is used. In this process a random ray of semi-infinite length must be created (O’Rourke 1998). The ray must be long enough to guarantee that it will exceed the boundaries of any tetrahedral element. The ray has a start point q and an end point r as shown in Fig. 6(b). If point q resides inside of the tetrahedron then the ray $\vec{q}\vec{r}$ will pass through an odd number of faces of the tetrahedron. If point q resides outside of the tetrahedron, but the ray still passes through the tetrahedron, then the ray will cross an even number of faces. The end point r of ray $\vec{q}\vec{r}$ can be placed randomly anywhere outside the dimensions of the structure. Every face of the tetrahedron is a plane that can be determined from its vertices as described by Young (1993).

$$Ax + By + Cz - D = 0 \tag{5}$$

The coefficients of the plane A, B, C and D may be determined using basic plane equations and three points on the plane $(x_2, y_2, z_2), (x_3, y_3, z_3)$ and (x_4, y_4, z_4) (Young 1993). The ray $\vec{q}\vec{r}$ must be scaled to

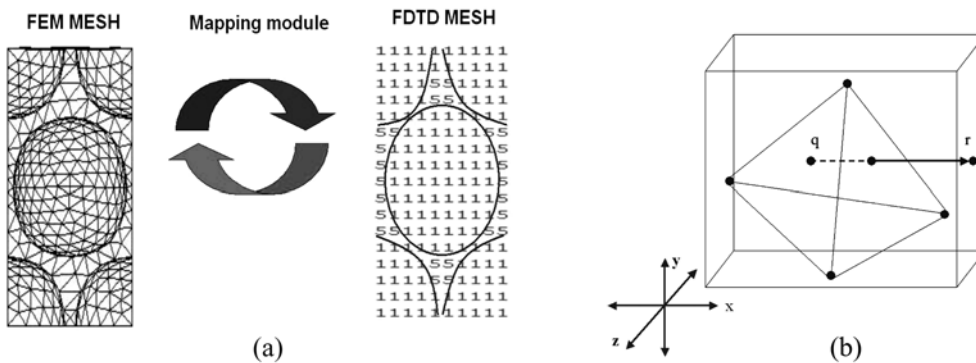


Fig. 6 Geometrical mapping module to relate coordinates of the FE mesh to that of the FDTD mesh (a) connecting FE and FDTD meshes of the inverse opal and (b) checking if a point resides inside a tetrahedron

determine if it crosses one of the faces of the tetrahedron. A unit vector normal to a plane \vec{N} is defined as: $\vec{N}=(A, B, C)$ where A, B and C are derived from Eq. (5). Any point on this plane such as $P(x_2, y_2, z_2)$ is subject to the equation where the dot product (\bullet) yields D :

$$(x_1, y_1, z_1) \bullet N = D \tag{6}$$

The ray is then scaled to determine its intersection with the plane. O'Rourke (1998) described the scaling variable, t , as

$$t = D - \frac{(q \bullet N)}{((r - q) \bullet N)} \tag{7}$$

When the denominator of Eq. (7) becomes zero, then the ray $\vec{q} \vec{r}$ is parallel to the plane of interest. When the numerator is zero, then point q is on the plane. For all other values of t the $\vec{q} \vec{r}$ ray is intersecting the plane. This process is repeated for all four planes forming the tetrahedron. Finally, to determine if q resides on one element vertex of the tetrahedron, three new tetrahedrons are formed from two vertices of the triangle and points q and r (O'Rourke 1998). The volumes of the tetrahedron are then calculated and the volume signs are evaluated.

2.4. Damage quantification using fuzzy set theory

It is well established that damage detection and recognition is usually based on observing changes in the damage feature with reference to the material response at healthy performance periods (Grandt 2004, Altunok, *et al.* 2007). In this paper, a new damage feature that relates the level of damage in the material to the reflectance spectra of a PhC sensor attached to the material surface is proposed. The proposed feature is based on comparing the reflectance spectra in damaged and undamaged/healthy states. Quantitative analysis of the damage begins with the assumption that multi-scale damage states in a material can be described by a finite number of overlapping fuzzy sets, A^i , such that $1 < i < N$ with N representing the total number of damage states.

The use of fuzzy set theory allows one to account for the fuzziness and nonspecificity types of uncertainty that are usually encountered in modeling damage. Nonspecificity expresses the uncertainty in damage due to lack of certain distinctions characterizing damage while fuzziness expresses the uncertainty in damage boundaries due to the lack of sharp boundaries separating damage levels (Klir 2006). To elaborate, it is recognized that such uncertainties in damage have always been a challenge that has hindered precise damage modeling due to the inherent overlapping in damage states and the absence of a method to measure damage (Lemaitre and Desmorat 2005, Reda Taha and Lucero 2005).

With the above definition, damage at the *ith* photonic response/damage state can be considered by the relative damage metric DM_i described after Ross (2004)

$$DM^i = D \left(1 - \left[\bigvee_{k=1}^n \left(A^H \wedge A^i \right) \wedge \bigwedge_{k=1}^n \left(\overline{A^H} \vee \overline{A^i} \right) \right] \right) \tag{8}$$

A^H and A^i are the fuzzy sets/vectors representing the healthy and *ith* damage state in the material, k is a counter and n is the total number of observations in each fuzzy vector, and \wedge and \vee are the minimum and maximum operators respectively. The damage metric DM is equal to one when the material is completely damaged (suffering from severe micro-damage), and is equal to zero when the material is undamaged (similar to healthy performance). D is the scale used to relate mechanical damage to the damage

metric. The damage scale D can be identified by calibration of the metric at several damage levels (submicron, micro, etc.). Calibration is necessary to allow the use of the technology for non-destructive testing applications. Such calibration is possible using constitutive modeling of the substrate material. Details on damage calibration process go beyond the scope of work here but can be found elsewhere (Sheyka 2008).

3. Case study

The purpose of this case study is to evaluate the integrated simulation environment for PhCs. The simulation environment begins with a FE model, which is mapped to an FDTD grid using a computational geometry approach. The FE model of PhC was developed in ANSYS® FE Code. The model represents a unit cell of an inverse opal PhC. The z-axis is parallel to the (111) direction of the FCC structure. The unit cell may be copied along any direction (x, y, z) to yield an entire inverse opal PhC. An isometric view of the FE model of the PhC is shown Fig. 7. The unit cell has dimensions of $0.707 \mu\text{m}$ by $1.22 \mu\text{m}$ by $1.7321 \mu\text{m}$. The PhC has a lattice constant of $0.707 \mu\text{m}$ and a submicron sphere radius of 353 nm . The inverse opal PhC matrix is made of polymethyl methacrylate (PMMA) and the periodic inserts are made of air spheres. Material properties of PMMA include Young's modulus 2.24 GPa , Poisson's ratio 0.35 and ultimate strength 53.8 MPa (Callister 2003). The model is assumed to be linear elastic and isotropic. Tetrahedron elements with 8 nodes and three-degrees of freedom at each node were used to model the PhC unit cell. The nodes may translate in the x, y and z directions respectively. The model contains $114,358$ elements and $23,946$ nodes. Due to symmetry conditions, the boundary conditions were only applied to four faces of the model. Three areas were given zero displacements in the direction normal to their plane. A given displacement was applied upon the face parallel to the y - z plane. The FE model output (i.e. the deformed shape of the unit cell) was directed to the FDTD model using the computational geometry module. The FDTD model was then used to simulate the photonic response of the PhC sensors.

Four cases representing three states of damage, in addition to the healthy case, were modeled. These include Case 1: representing the healthy substrate, Case 2: PhC sensor observing local uniform strain of

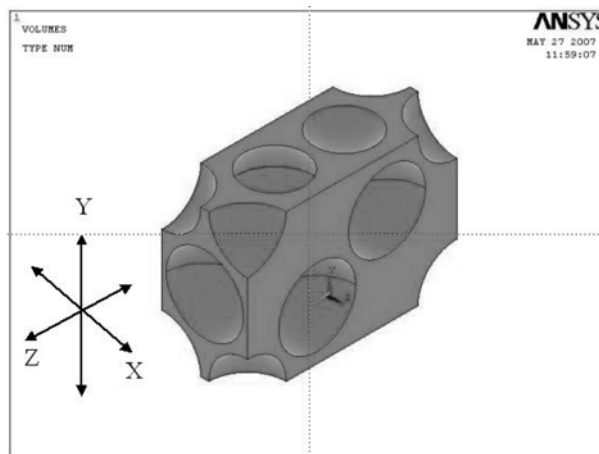


Fig. 7 Isometric view of inverse opal unit cell

(5%) at the substrate, Case 3: PhC sensor observes significantly high local uniform strain of (20%) at the substrate and Case 4: PhC sensor observes non-uniform local strain field due to damaged substrate. Strain distributions associated with Cases 2, 3 and 4 are shown in Fig. 8.

In each case, a unit cell was modeled in using the FE method and the geometry of the deformed PhC was mapped and transferred to the FDTD method using the computational geometry module. The FDTD model simulated the PhC structure subjected to the strain fields for the different simulation cases. The PhC structure consists of 10 unit cells (7 microns in length) in the direction of strain application. The PhC sensor photonic response was then simulated using the FDTD method. The spectral response of each case was then compared to Case 1 and the damage metric DM to quantify damage in the substrate was computed.

4. Results and discussion

The FE model developed in this study was capable in simulating the behavior of the PhC sensor unit cell. The bandgap is the region of the spectral where 100% of the photons are reflected. Fig. 9 shows that the reflectance spectral of the PhC sensor for Case 1 modeled using the FE-FDTD integrated approach showed a bandgap between 68 and 78 THz (Terahertz). It can be also observed in Fig. 9 that when a PhC sensor experienced uniform local strains of 5 and 20% (Case 2 and Case 3), shifts in the bandgap towards low frequency were observed. This is due to the scale invariance of Maxwell's equations underlying PhC physics (Joannopoulos, *et al.* 2008). As shown in Fig. 9, this shift is much more pronounced in Case 3 as compared with Case 2 due to the relatively local uniform strain in Case 3 (20%). As the substrate becomes damaged the spectral response begins to loose the overall shape of the bandgap. Case 4 with of the non-uniform strain shown in Fig. 7 resulted in a significant shift in the bandgap as shown in Fig. 9. It is important to note that the 5 and 20% strains in the PhC (Cases 2 and 3) represent deformation magnitudes of 350 nm (nanometer) and 1.4 μm (micrometer) in the substrate respectively. This represents the significantly high resolution of the PhC sensor. Finally, the non-

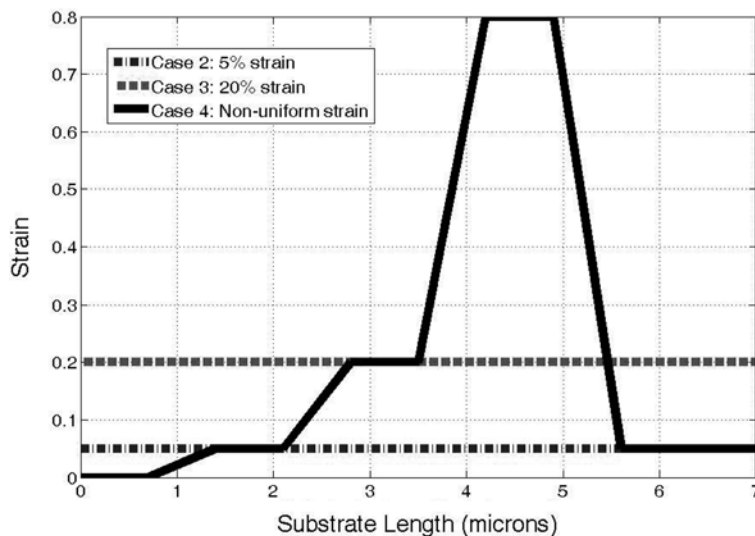


Fig. 8 Strain distributions for Cases 2, 3 and 4

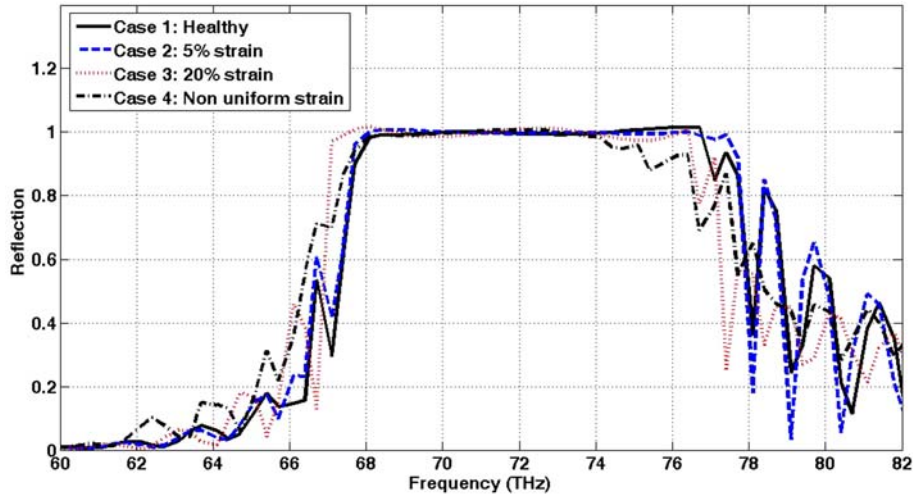


Fig. 9 Reflectance spectral for the four case studies showing the effect of damage on bandgap profile of PhC sensors

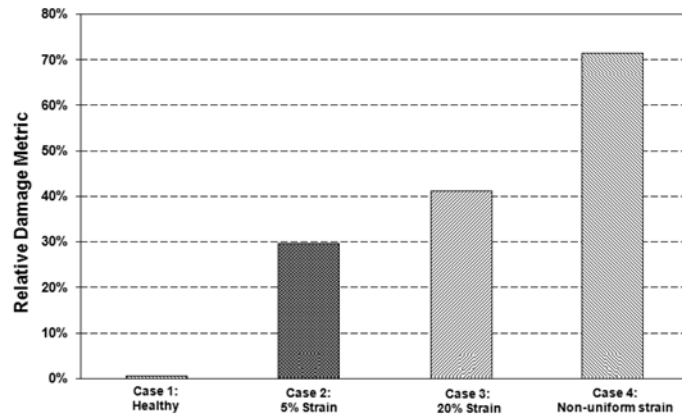


Fig. 10 Relative damage metric (DM) values for all cases

uniform strain represented in Case 4 results in a deterioration of the bandgap profile specially at the high frequency region > 68 THz as shown in Fig. 9.

The bandgap profiles shown in Fig. 9 were used to compute the relative damage metric DM for the three cases as shown in Fig. 10. The damage metric shows a distinct difference between the undamaged case: Case 1: ($DM = 0$), the cases with uniform local strains, Case 2 ($DM = 0.29$), Case 3 ($DM = 0.41$) and Case 4 ($DM = 0.71$). DM values indicate relatively medium damage in Cases 2 & 3 and relatively severe damage in Case 4. It is important to realize that the damage metric only provides an indication of relative damage rather than absolute measure of damage. Realizing absolute measure of damage requires calibration of the damage metric using mechanical testing (Sheyka 2008). The results prove the sensitivity of the PhC sensor to detect micro-damage in a substrate adhered to it.

Combining the PhC technology with the proposed damage quantification method showed promising results indicating the ability of the proposed PhC sensor to detect and quantify micron and submicron damage in materials. Experimental validation of the proposed simulation is necessary to prove the

ability of the PhC sensor and is provided elsewhere (Sheyka 2008).

5. Conclusion

This article provides a proof of concept showing the possible use of new photonic sensors based on PhC technology for micro-damage detection and quantification. A simulation approach, integrating the FE method and the FDTD method by means of a computational geometry approach is presented. In addition, a method to quantify micro-damage detection in substrates adhered to the photonic sensors is introduced. Numerical simulation results confirmed the PhC sensors ability to detect and quantify multiple damage cases in an inverse opal PhC attached to a PMMA bar. The simulation also demonstrated the sensitivity of the photonic sensor. Combining the PhC technology and the proposed damage quantification technique provides a new sensing technology to probe damage at micron and submicron scales. A new boundary for micro-damage detection not reported before is presented.

Acknowledgements

Research described in this work has been funded by Sandia National Laboratories (SNL). Sandia is a multi-program laboratory operated by Sandia Corporation, a Lockheed Martin Company, for the United States Department of Energy's National Nuclear Security Administration under contract DE-AC04-94AL85000. The authors acknowledge this support. Funding to the first author by Defense Threat Reduction Agency (DTRA) through UNM strategic partnership program is strongly appreciated.

References

- Adams, D.E. (2007), *Health Monitoring of Structural Materials and Components*, John Wiley & Sons, West Sussex, UK.
- Altunok, E., Reda Taha, M.M. and Ross, T.J. (2007), "A Possibilistic approach for damage detection in structural health monitoring", *J. Struct. Eng.* ASCE, **133**(9), 1247-1256.
- Biswas, R., El-Kady, I., Lin, S.Y. and Ho, K.M. (2003), "Enhanced complete photonic band gap in the optimized planar diamond structure", *Photonics Nanostruct.*, **1**(13), 251-253.
- Callister Jr., W.D. (2003), *Material Science and Engineering an Introduction*, John Wiley and Sons, Inc., NJ.
- Doebling, S.W., Farrar, C.R., Prime, M.B. and Shevitz, D.W. (1996), "Damage identification and health monitoring of structural and mechanical systems from changes in their vibration characteristics: a literature review", Los Alamos National Laboratory report LA-13070-MS.
- El-Kady, I. (2002), "Modeling of Photonic Band Gap Crystals and Applications", PhD Thesis, Iowa State University, Ames, IA.
- El-Kady, I., Farfan, B.G., Rammohan, R. and Reda Taha, M.M. (2008), "Photonic Crystal High-Efficiency Multispectral Thermal Emitters", *Appl. Phys. Lett.*, **93**(15), 153501.
- Escobar, J.A., Sosa, J.J. and Gomez, R. (2005), "Structural damage detection using the transformation matrix", *Comput. Struct.*, **83**, 357-368.
- Fleming, J.G., Lin, S.Y., El-Kady, I., Biswas, R. and Ho, K.M. (2002), "All-metallic three-dimensional photonic crystals with a large infrared bandgap", *Nature*, **417**(6884), 52-55.
- Grandt, A. (2004), *Fundamentals of Structural Integrity*, John Wiley & Sons, NY.
- Joannopoulos, J.D., Villeneuve, P.R. and Fan, S. (1997), "Photonic crystals: putting a new twist on light", *Nature*, **386**, 143-149.

- Joannopoulos, J.D., Johnson, S.G., Winn, J.N. and Meade, R.D. (2008), *Photonic Crystals: Molding the Flow of Light*, 2nd ed., Princeton University Press, Princeton, NJ.
- Kessler, S.S. and Spearing, S.M. (2002), "Design of a piezoelectric based structural health monitoring system for damage detection in composite materials", *Proc. of the SPIE Symposium on Smart Structures and Materials*, March 2002.
- Klir, G.J. (2006), *Uncertainty and Information: Foundations of Generalized Information Theory*, John Wiley & Sons, NJ.
- Lemaitre, J. and Desmorat, R. (2005), *Engineering Damage Mechanics: Ductile, Creep, Fatigue and Brittle Failures*, Springer, NY.
- Lin, J.G., Fleming, D.L., Hetherington, B.K., Smith, R., Biswas, K.M., Ho., M.M., Sigalas, W., Zubrzycki, S.R., Kurtz, S.R. and Bur, J.A. (1998), "A three-dimensional photonic crystal operating at infrared wavelengths", *Nature*, **3(94)**, 251-253.
- Lin, L.L., Li, Z.Y. and Ho, K.M. (2003), "Lattice symmetry applied in transfer-matrix methods for photonic crystals", *J. Appl. Phys.*, **94(2)**, 811.
- Logan, L.D. (2002), *A First Course in the Finite Element Method*, Thomas Learning, Inc., NY.
- O'Rourke, J. (1998), *Computational Geometry in C*, Cambridge University Press, NY.
- Reda Taha, M.M., Noureldin, A., Lucero, J.L. and Baca, T.J. (2006), "Wavelet transform for structural health monitoring: a compendium of uses and features", *Struct. Health Monit.*, **5(3)**, 267-295.
- Reda Taha, M.M. and Lucero, J. (2005), "Damage identification for structural health monitoring using fuzzy pattern recognition", *Eng. Struct.*, **27(12)**, 1774-1783.
- Ross, T.J. (2004), *Fuzzy Logic with Engineering Applications*, John Wiley & Sons, Chichester, UK.
- Sigalas, M., Soukoulis, C.M., Chan, C.T. and Turner, D. (1996), "Localization of electromagnetic waves in two-dimensional disordered systems", *Physics Review B*, **53**, 8340.
- Sohn, H., Worden, K. and Farrar, C.R. (2003), "Statistical damage classification under changing environmental and operational conditions", *J. Intel. Mat. Syst. Str.*, **13(9)**, 561-574.
- Sheyka, M. (2008), "Analytical and Experimental Investigations of Photonic Crystals for Sub-Micron Damage Detection", M.Sc Thesis, Department of Civil Engineering, University of New Mexico, Albuquerque, NM.
- Talreja, R. (1994), *Damage Mechanics of Composite Materials*, Elsevier Science, NY.
- Ward, A.J. and Pendry, J.B. (1998), "Calculating photonic Green's functions using a nonorthogonal finite-difference time-domain method", *Physics Review B.*, **58(11)**, 7252-7259.
- Worden, K. and Dulieu-Barton, J.M. (2004), "An overview of intelligent fault detection in systems and structures", *Struct. Health Monit.*, **3(1)**, 85-98.
- Young, C.E. (1993), *Vector and Tensor Analysis*, Marcel Dekker, NY.